SF2A 2021
A. Siebert, K. Baillié, E. Lagadec, N. Lagarde, J. Malzac, J.-B. Marquette, M. N'Diaye, J. Richard, O. Venot (eds)

THE SOLAR NEIGHBOURHOOD AS SEEN BY GAIA

C. Reylé[1]

Abstract. The *Gaia* astrometric space mission with all sky parallax measurements for about 1.5 billion objects offers the means to complete volume-limited samples with large distance limits. The *Gaia* Catalogue of Nearby Stars (GCNS) is a clean and well-characterized catalogue of objects within 100 pc of the Sun produced from the *Gaia* Early Data Release 3 (EDR3). It has 331 312 entries that is an increase by an order of magnitude with respect to the most complete nearby star census prior to the *Gaia* mission. We briefly show how the catalogue was constructed and why it was not possible before *Gaia EDR3*. Several scientific results were drawn from the catalogue, we here focus on the kinematics properties. We also give a short overview of the 10 pc sample, a by-product of the GCNS.

Keywords: Galaxy: solar neighbourhood, Galaxy: stellar content, parallaxes, kinematics

1 The Gaia Catalogue of Nearby Stars

The *Gaia* Catalogue of Nearby Stars Stars (hereafter GSS21, Gaia Collaboration et al. 2021b) is one of the scientific demonstration papers that have been issued at the same time of the third data release 3 (hereafter *Gaia* EDR3, Gaia Collaboration et al. 2021a) of the *Gaia* mission (Gaia Collaboration et al. 2016). The GCNS is an attempt to make a census of all stars within 100 pc of the Sun using *Gaia* EDR3 to find their distance, motion, magnitude and colour. Such catalogue is important since it provides a calibrating point where unbiased, homogeneous and precise data on all objects can be used to extend our nearby understanding to the whole Galaxy. The 100 pc limit has been chosen because one can expect to have all stars within this volume: GSS21 estimated a completness of 92% for all stars (up to the spectral type M9).

Such a task is not easy to do with the previous *Gaia* data release (hereafter *Gaia* DR2, Gaia Collaboration et al. 2018). It requires a very high astrometric precision, now reached with *Gaia* EDR3, to disentangle between false and true objects. Because *Gaia* measured parallaxes for 1.5 billion stars, even if a tiny proportion of them have a bad astrometric solution, they can scatter on the large parallax tails (both on the positive and negative sides, see Figure 1, left panel) and make more numerous spurious nearby stars than real ones.

Even with the improved astrometry in *Gaia* EDR3, it is not trivial to construct a volume limited catalogue. The simple cut in parallax, $\varpi > 10$ mas, is not enough. Spurious astrometric solutions remain, in particular in crowded regions or for binary stars (*Gaia* EDR3 has a single star astrometric solution). GCNS was constructed with a random forest classification using two training set of objects with "good" and "bad" astrometric solutions. Bad objects are selected with $\varpi < -8$ mas. Good objects are selected outside the Galactic plane, have consistent photometry in *Gaia* (G, $G_{\rm RP}$) and 2MASS (Skrutskie et al. 2006) bands (J, H, K_S), and $\varpi > 8$ mas. All features used for classification are astrometric. The procedure returns a probability of reliable astrometry.

In fine, 625 171 objects are rejected and 331 312 objects constitute the GCNS (see Section 2.1 in GSS21 for a complete description of the classification). A large part of rejected objects are in crowded regions or would have an absolute magnitude M_G around 15 (see figures 1 and 2 in GSS21), which is probably a contamination due to bad solutions for the faintest stars ($G = 20$), e.g. lowest signal-to-noise, near the 100 pc limit where $G = 20$ converts to $M_G = 15$. The same classification procedure have been applied in *Gaia* DR2. Figure 1, right panel, shows the parallax distribution for all objects and only good objects, in *Gaia* DR2 and *Gaia* EDR3. It illustrates that even this classification cannot remove all false entries in *Gaia* DR2(15 entries with $\varpi > 500$ mas remain in *Gaia* DR2, whereas *Gaia* EDR3 has only one, Proxima Centauri).

[1] Institut UTINAM CNRS UMR6213, Université Bourgogne Franche-Comté, OSU THETA Franche-Comté Bourgogne, Observatoire de Besançon, BP1615, 25010 Besançon Cedex, France

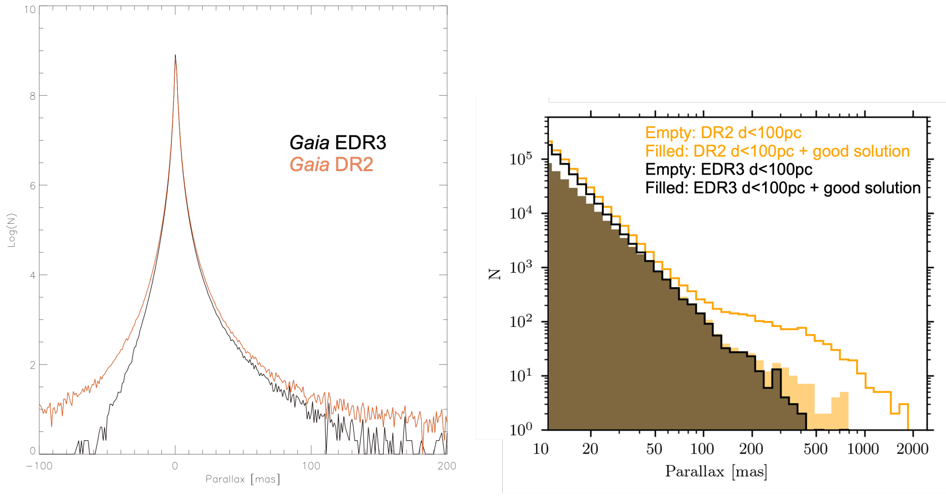

Fig. 1. Left: number of stars (in logarithmic scale) as a function of parallax in *Gaia* DR2 (orange) and *Gaia* EDR3 (black). Right: Zoom on the large parallax tail, showing the *Gaia* DR2 (orange) and *Gaia* EDR3 (black) content before (empty) and after (filled) the random forest classification.

Several examples of scientific exploitation of the GCNS are given in GSS21 (see their Section 5), on the luminosity function, the local kinematics, the Hyades cluster, the ultra-cool dwarfs, the white dwarfs, the unresolved and wide binaries. We here focus on the exploration of the local kinematical plane.

2 The local kinematics from GCNS

In the GCNS, 74 281 stars have a radial velocity in *Gaia* EDR3 (22% of the full GCNS). For those it was possible to compute the (U, V, W) cartesian velocities in the Galactic frame. The resulting Toomre diagram is shown in Figure 2, upper left panel.

Even in this very local sample, the kinematics plane is highly structured in the thin disc, probably due to dynamical effects attributed by several studies to resonance of the bar or linked to the spiral structure (Antoja et al. 2012; Monari et al. 2017; Hunt et al. 2018; Michtchenko et al. 2018).

The nearby halo is clumpy as well. Twelve stars with kinematics similar to *Gaia* Enceladus, a major event experienced by the Milky Way (Helmi et al. 2018) are highlighted in Figure 2, upper left panel. The most extreme star in the Toomre diagram is GJ 725 AB, a twin pair of chemically anomalous stars with a probable extragalactic origin (Reggiani & Meléndez 2018).

The orbital parameters were computed using the online tool Gravpot16*. The Galactic potential we used is a non-axisymmetric potential including the bar, developed by Fernandez-Trincado (2017)†. Gravpot16 is based on a Galactic gravitational potential driven by the Besançon Galaxy Model mass distribution. It includes an axisymmetric component (discs, stellar halo, dark halo, interstellar medium) whose potential computation is described by Bienaymé et al. (1987), and a non axisymmetric component (boxy bar, described in Robin et al. 2012) whose potential is computed via Pichardo et al. (2003) method.

Assuming a bar mass of 10^{10} $M_{\odot}$, a bar pattern speed of 43 km s^{-1} kpc^{-1}, a bar angle of 20°, we compute various orbital parameters: pericentric and apocentric distances, inclination, ellipticity, orbital energy, Jacobi constant, angular momentum, etc. We explore the orbital energy vs Jacobi constant plane‡ to define several groups, as proposed by Fernández-Trincado et al. (2020). It is shown in Figure 2, lower left panel.

We tentatively interpret this diagram. Most of the stars are in the disc and shown by the orange density-scaled region. The clump of twelve stars (blue dots) lies in the region expected for stars dynamically associated with *Gaia* Enceladus, being either merger stars or stars heated by the it. Sixty stars (orange squares) located

*https://gravpot.utinam.cnrs.fr/

†http://theses.fr/s108979

‡The Jacobi energy considers the bar pattern speed, potential energy, and kinetic energy. The total orbital energy is the kinetic plus potential energy.

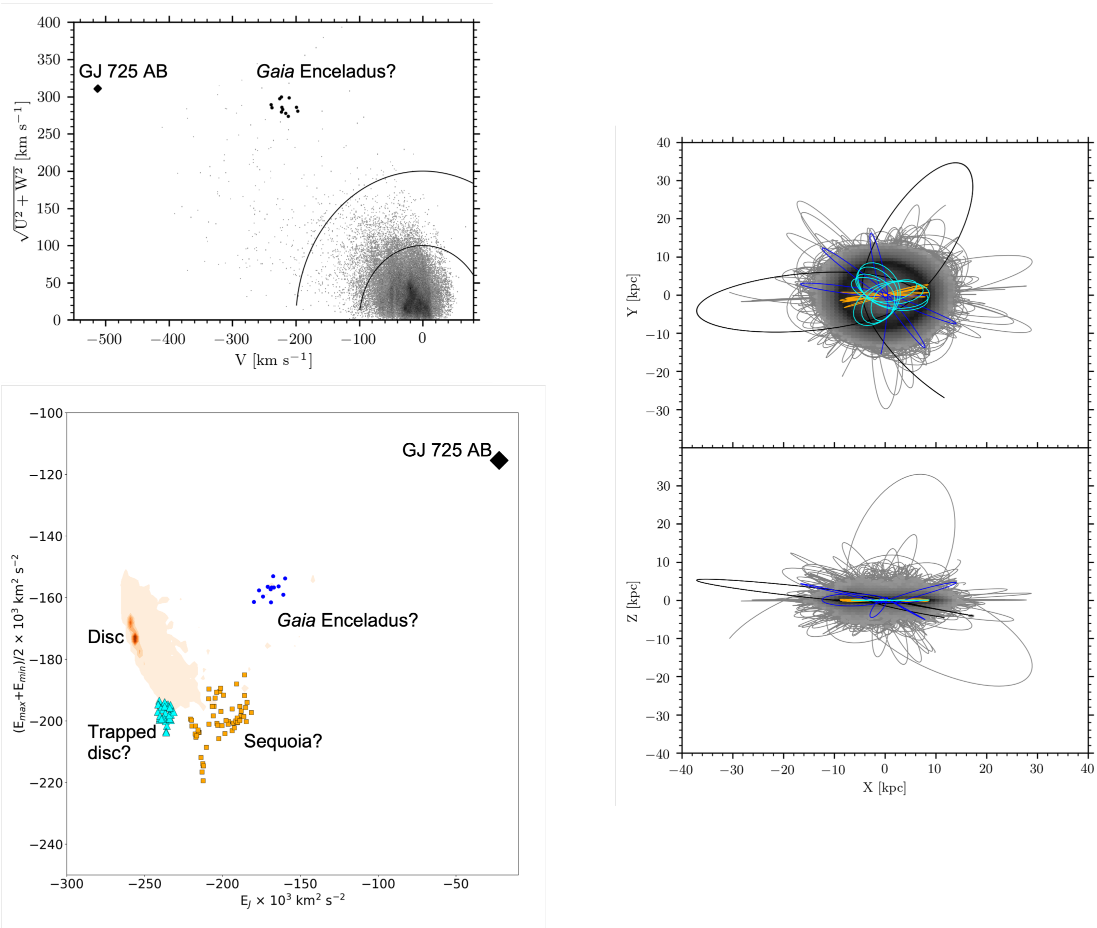

Fig. 2. Upper left: Toomre diagram for all the GCNS entries with a radial velocity in *Gaia* EDR3. The circles indicatively delineate thin-disc, thick-disc, and halo stars. Lower left: orbital energy vs Jacobi energy for all the GCNS entries with a radial velocity in *Gaia* EDR3. Courtesy of José G. Fernández-Trincado. Right: Orbits over 1 Gyr (forward), depicted on a face-on (top) and an edge-on (bottom) view. The colours refer to the objects highlighted on the left panel.

in the low-energy region could be associated to Sequoia, another major merger event (Myeong et al. 2019). The "hook" sample of 40 stars (cyan triangles) in the low-energy tail of the disc could be disc stars trapped in resonance with the bar structure. Further analysis of these groups should be done by cross-identification with spectroscopic surveys, or spectroscopic follow-up of the kinematical "outliers" for chemical characterisation.

Orbits are integrated over 1 Gyr, forward, in the referential frame of the Galaxy[§]. They are shown in Figure 2, right panel. The most numerous disc stars, such as the Sun, populate the circular orbits in the Galactic plane($Z = 0$). Halo stars have higher eccentricities and inclinations.The central part of the (X, Y) plane is populated by the orbits of stars coming from (or going to) the central regions of the Galaxy.

3 The 10 pc sample

As a by-product of the GCNS, we compiled all stars and brown dwarfs within 10 pc observable by *Gaia* and compare it with the GCNS as a quality assurance test. We further complement the list to get a full 10 pc census, including bright stars, brown dwarfs, and vetted exoplanets. The resulting catalogue contains 540 stars, brown dwarfs, exoplanets in 339 sytems, and is the as volume-complete as possible list from current knowledge (Reylé et al. 2021). The colour-absolute magnitude diagram is shown in Figure 3, coloured as a function of spectral type, superimposed with the GCNS (grey dots). It provides benchmark stars to define calibration samples, and to test the quality of the forthcoming Gaia releases.

[§]An animation of these orbits can be seen on `https://www.youtube.com/watch?v=k9pHGhNtyPk&ab_channel=ESAGaiaMission`

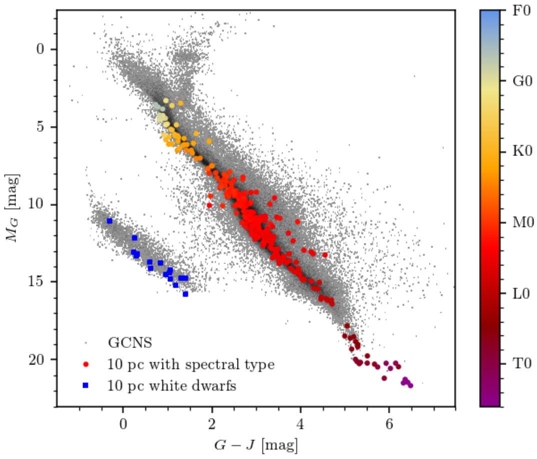

Fig. 3. Colour-absolute magnitude diagram of the 10 pc sample, superimposed on the GCNS (grey dots). The colour bar indicates the spectral type. White dwarfs are in dark blue. From Reylé et al. (2021).

4 Conclusions

The *Gaia* Catalogue of Nearby Stars offers a clean, homogeneous and precise sample of the 100 pc sphere, allowing a detailed kinematics study (but not only). It contains a large diversity of stars and show that our "today" neighbours are from all the parts of the Galaxy, including the innermost regions. The *Gaia* next data release in 2022 will provide radial velocities for over 50% of the GCNS, allowing the computation of more more orbits and charaterisation of nearby streams, but also astrophysical parameters for complementary chemical characterisation. It will also improve the astrometric solution of binary stars, and will allow to update the very nearby, 10 pc sample.

The *Gaia* Catalogue of Nearby Stars, the 10 pc catalogue, and outreach material can be found on `https://gucds.inaf.it/`.

References

Antoja, T., Helmi, A., Bienayme, O., et al. 2012, MNRAS, 426, L1
Bienaymé, O., Robin, A. C., & Creze, M. 1987, A&A, 180, 94
Fernandez-Trincado, J. 2017, PhD thesis, University Bourgogne-Franche-Comté, France, http://theses.fr/s108979
Fernández-Trincado, J. G., Chaves-Velasquez, L., Pérez-Villegas, A., et al. 2020, MNRAS, 495, 4113
Gaia Collaboration, Brown, A. G. A., Vallenari, A., et al. 2018, A&A, 616, A1
Gaia Collaboration, Brown, A. G. A., Vallenari, A., et al. 2021a, A&A, 649, A1
Gaia Collaboration, Prusti, T., de Bruijne, J. H. J., et al. 2016, A&A, 595, A1
Gaia Collaboration, Smart, R. L., Sarro, L. M., et al. 2021b, A&A, 649, A6
Helmi, A., Babusiaux, C., Koppelman, H. H., et al. 2018, Nature, 563, 85
Hunt, J. A. S., Hong, J., Bovy, J., Kawata, D., & Grand, R. J. J. 2018, MNRAS, 481, 3794
Michtchenko, T. A., Lépine, J. R. D., Pérez-Villegas, A., Vieira, R. S. S., & Barros, D. A. 2018, ApJ, 863, L37
Monari, G., Kawata, D., Hunt, J. A. S., & Famaey, B. 2017, MNRAS, 466, L113
Myeong, G. C., Vasiliev, E., Iorio, G., Evans, N. W., & Belokurov, V. 2019, MNRAS, 488, 1235
Pichardo, B., Martos, M., Moreno, E., & Espresate, J. 2003, ApJ, 582, 230
Reggiani, H. & Meléndez, J. 2018, MNRAS, 475, 3502
Reylé, C., Jardine, K., Fouqué, P., et al. 2021, A&A, 650, A201
Robin, A. C., Marshall, D. J., Schultheis, M., & Reylé, C. 2012, A&A, 538, A106
Skrutskie, M. F., Cutri, R. M., Stiening, R., et al. 2006, AJ, 131, 1163